Transactions on Additive Manufacturing Meets Medicine
Trans. AMMM, 2024, Vol. 6, No 1, Article ID 1884, 8 Pages

Infinite Science Publishing

Original Research Article

Modeling technique selection for cranial reconstruction

P. Jindal[1], M. Juneja[1*], A. Goel[1], Y. Reinwald[2,3*], J. Watson[4], R. O'Connor[4], and P. Breedon[2,3]

[1]*University Institute of Engineering and Technology, Panjab University, Chandigarh, India*
[2]*School of Science and Technology, Department of Engineering, Nottingham Trent University, Nottingham UK*
[3]*Medical Technology Innovation Facility, Nottingham Trent University, Nottingham UK*
[4]*Nottingham University Hospital, Nottingham UK*
[*] *Corresponding authors, emails: yvonne.reinwald@ntu.ac.uk, mamtajuneja@pu.ac.in,*

Abstract: *Skull reconstruction using cranial implants is essential to protect intracranial structures and to restore cerebral hemodynamics when accidents, disease, or cancer cause craniofacial anomalies. Cranioplasty aims to protect the brain inside the skull and to achieve a desired cosmetic result. With the development of digital 3D technology, Patient-Specific Implants (PSI) have been widely used for surgical correction of congenital, post-traumatic, or post-surgical abnormalities. PSIs must mimic the natural structure of bones, be biocompatible, lightweight, and stress resistant. Interface joints and fastening mechanisms are essential for a robust connection to the injured cranium. With an emphasis on four typical cranial defects, namely small frontal, big lateral, large bilateral, and zygomatic bone defects, this study examines the use of several methodologies for PSI construction. Defect-specific implant fabrication is commonly performed using digital subtraction after mirror imaging on the normal side of the skull or shape-based interpolation. To compare both methods, we used the Edge Gap Factor (EGF), defined as the ratio of the interpolated implant's mode edge deviation to that of the mirrored implant. An EGF < 1 indicates superior performance of the interpolation method, while an EGF > 1 indicates superior performance of the mirroring method. Both methods perform similarly when EGF = 1. Here, we verify if the gap is homogenous and whether the spacing between neighboring surface clusters is constant during the gap length through the analysis of EGF. For each of the four defect cases, the two implants that were regenerated utilizing both procedures had their gap sizes compared to identify the best match. Therefore, the degree to which the implant fills the defect was assessed by measuring the gaps between the implant and the skull interface. This study provides guidelines for the best implant generation process, considering four distinct cranial deformities that account for most skull defects.*

I. Introduction

The primary procedure used in neurosurgery to treat a skull vault defect is called cranioplasty, which involves implanting bone or non-biological materials like metal or plastic plates [1]. Traumatic brain injuries (TBI) are a major cause of mortality and disability among all trauma-related injuries in the globe, accounting for one-third to one-half of these deaths [2]. In addition to trauma, cranial abnormalities or deformities can come from illness, congenital anomalies, or abnormal growths such as tumors [3,4,5,6]. In certain circumstances, a cranioplasty may be required to repair or replace the lost section of the skull and restore brain function. Craniectomy and cranioplasty are frequently performed together as complimentary operations [7]. A cranioplasty can be performed using a variety of techniques, depending on the patient's individual needs, the size and location of the cranial defect, and the surgeon's skill and preference [8]. Autograft, allograft, computer-aided design, and implant manufacturing (CAD/CAM) or custom-made implants are some of the most prevalent procedures for doing cranioplasty [9].

According to reports, large titanium implants have been used widely to treat cranial abnormalities. Because of the variation in Young's modulus, thick titanium implant cause stress-shielding effects at the interface between the implant and the host tissue. Furthermore, Titanium weighs 1.6 times more than the restored bone [10]. Novel porous cranial implants improve healing by reducing stress-shielding issues and by promoting quicker tissue in-growth and vascularization [11]. Increased porosity and pore size can promote bone development but may reduce implant strength significantly [12]. The creation of porous titanium and related alloys has historically involved the use of several processes, including casting, fiber deposition, and powder sintering [13,14,15].

However, there are certain drawbacks to each of these methods, including irregular porosity, contaminants, and unreliable interconnectivity. From a manufacturing perspective, it is frequently necessary to quickly and effectively build a patient-specific porous implant [11]. Patient-specific implants (PSIs) have become a viable option for treating complicated geometries in the maxilla and mandible. Nowadays, PSIs are used in many areas of oral and maxillofacial surgery, including orthognathic surgery, complete joint replacement, reconstruction of the facial skeleton, and temporomandibular joint (TMJ). The use of PSI and personalized implant fittings result in shorter recovery periods [16]. Through thorough examination of the patient's condition, physicians ensure that the right implant design and material are chosen, and that they make well-informed judgments about the best procedure to use [17].

Most cranial implant designs employ the symmetric technique of manufacture for symmetrical abnormalities. However, creating cranial implants for complicated malformations and asymmetrical abnormalities is more challenging. Large lesions necessitate a specialized construction technique. Curvatures at different sections have been utilized to simulate cranial implants recently; an algorithm based on curvature was employed to fix a big defect in the skull [18]. Such techniques allow for greater precision in terms of the implant shape and allow surgeons to better visualize the defect. This research employs a variety of implant generating approaches, including commonly used methods such as digital subtraction after mirror imaging on the normal side of the skull [19,20,21], and shape-based interpolation [22].

Marreiros et al. created a CAD program that uses the Radial Basis Function's interpolation characteristics to create a tailored implant for big cranial lesions (>100 cm^2) [23]. Also, in this paper we utilize Edge Gap Factor (EGF) [24] and present recommendations based upon the EGF in 4 cases, each presenting with a unique cranial defect. Surface clusters frequently have a fileted outside border with a certain radius. The shortest path between the edge filets of two nearby surface clusters is known as the gap. The viewpoint determines how big or small the gap seems to be. The gap's appearance from various angles and homogeneity can vary. If the spacing between neighboring surface clusters is constant over the gap length, these features can both be examined with this analysis function.

II. Materials and methods

II.I Creation of 3D models from DICOM files

Four individuals with various cranial abnormalities had their CT scans (computerized tomography) retrieved from Nottingham University Hospital as a DICOM (.dcm) file. Medical data may be imaged, stored, and sent electronically using the Digital Imaging and Communications in Medicine (DICOM) standard. It enables the sharing of medical data among computers, devices, and equipment. Computed Tomography (CT) scans were used to create pictures of a damaged skull. Using the segment editor and volume rendering tool in 3D slicer, the cranial volume was produced. Different structures of interest can be specified using the segment editor module [25]. To identify the problem and carry out additional processing, it enabled us to isolate the skull bone from surrounding tissue.

The threshold effect was used after segment creation to distinguish the bone from other tissue segments. The Hounsfield unit (HU) requires us to designate a radio intensity window to meet the threshold [26]. The skull bone would be around +1000(HU) at standard CT x-ray beam energy of 120–140kV [27].

On an individual basis, the threshold window's HU range may need to be manually adjusted. Manual paint and erase tools are used for additional refining once the threshold range has been established. The produced skull volume can be stored as a standard tessellation language (STL) file [28]. Surface triangular facet representations are found in STL files, which are generated by 3D modeling applications. For fast prototyping and production systems, this format is regarded as a standard data entry [29].

II.II Design of cranial implant using mirroring

With Autodesk Meshmixer (V3.5.474, Autodesk) a mirrored implant is created when an STL file has been received. To begin with, Meshmixer imports the STL file for this purpose. Next, any unnecessary geometry is removed from the model.

A mirrored version of the skull is then prepared using the mirroring tool. Its counterpart is positioned so that the original skull's defect precisely overlaps the matching, healthy area of the mirrored skull. If the skull is fully symmetrical, there should be a perfect overlap between the areas. The Align tool in Meshmixer was used to get a tighter overlap following a crude manual alignment. The implant was then acquired using Boolean subtraction. The implant was meticulously shaped by hand to precisely match the defect [11,30]. The sculpting tools in Meshmixer were utilized to manually correct any residual protrusions or gaps.

II.III. Design of cranial implant using Interpolation

The 3D Slicer (v5.0.2, The Slicer community), software's volume rendering module was used to import DICOM information to create an interpolated implant. A 3D model of the defective skull was produced in this module using the DICOM data, as seen in Figure 1.

This model was used to examine the defect in three-dimensions. Next, as shown in Figure 2, the three views of the DICOM files, namely axial, sagittal, and coronal, were

utilized to determine the optimal geometry for analyzing the whole cranial defect.

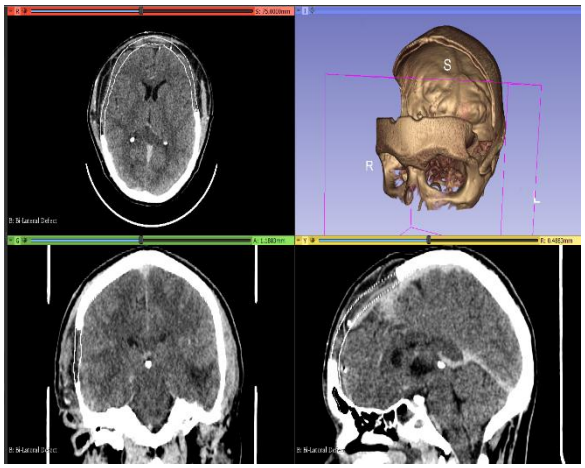

Figure 1: Volume rendering of the DICOM files to create a 3D skull model.

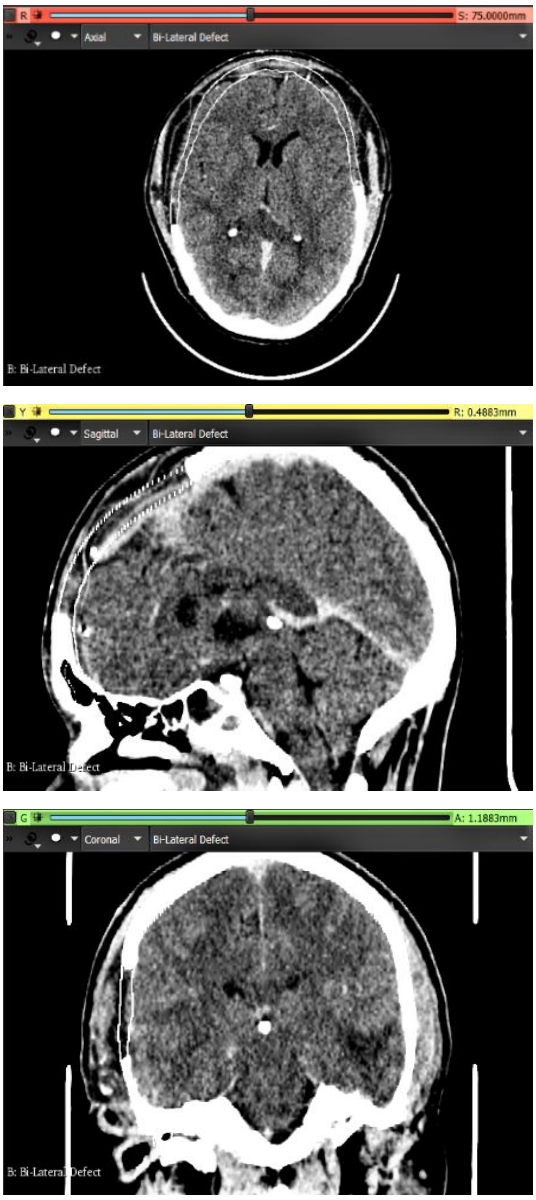

Figure 2: Different views of the damaged skull, top) Axial View middle) Sagittal View bottom) Coronal view.

Using the Segment Editor module, a new segment was created, once the problem was correctly spotted in one of the three views. After that, the newly produced section was altered to recreate the defective skull in the chosen perspective.

An axial, sagittal, or coronal view iteration is referred to as a slice. The missing skull's contour was created on every fifth slice using the Segment Editor module's Paint tool. The brush diameter was adjusted to 2% to merge the contour that is formed with the thickness of the existing bone. Once all of these settings were made, the two extreme spots, or slices, where the fault begins and ends, were identified. Then, as shown in Figure 3, a contour was drawn on every fifth slice of the Sagittal view. In this study the defect is best evaluated in this view. The contour was drawn starting from one extreme slice and moving towards the opposite extreme.

Figure 3: Creating the contour of the missing skull part.

In order to ensure optimal implant fitting during surgery with the least amount of rework, the gap was designed with that clearance in mind. Therefore, 52 slices with 4 slices step size in between each subsequent slice were successfully contoured.

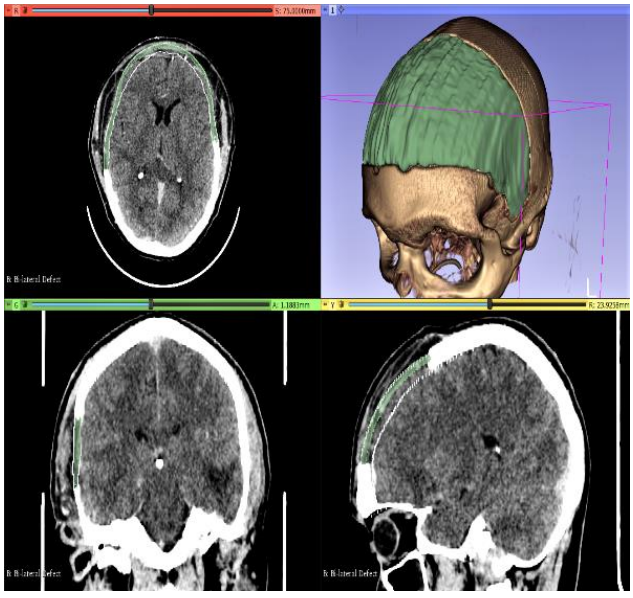

Figure 4: Interpolated implant using fill between slices command.

Upon completion, the contour's trace may be examined from the last two perspectives to confirm that its dimensions and form are correct. Using the fill-between-slices function of the Segment Editor module, the interpolation was then initiated as seen in Figure 4.

For the next step the smoothing feature was applied to the interpolated implant. Initially, the implant's pores and holes were sealed by setting the smoothness parameter to Closing (fill holes). The final smoothed implant is seen in Figure 5 after the smoothing setting was changed to Joint Smoothing.

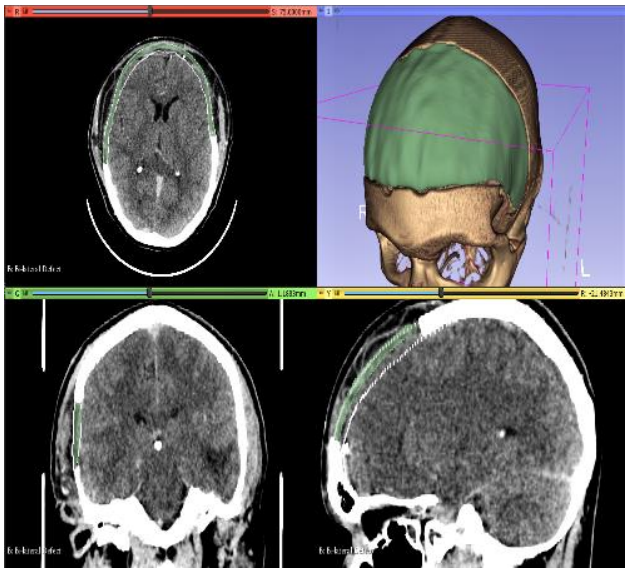

Figure 5: Implant after smoothing.

Following the export of the implant in STL format, the implant and the Skull model were loaded into Autodesk Meshmixer to verify correct alignment. Manual changes were then undertaken in accordance with surgical standards [24].

III. Results

III.I. Case 1- Small frontal defect

When the defect is localized and non-sagittal, both interpolation and mirroring can be used for reconstruction as shown in Figure 6. These methods leverage the surrounding intact bone structure to estimate the missing regions accurately.

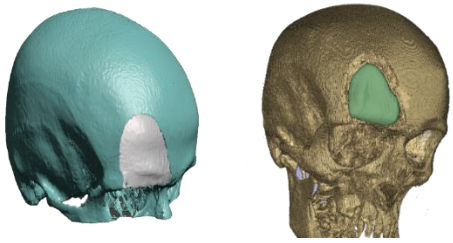

Figure 6: Implant for small frontal defects using top) mirroring and bottom) interpolation.

III.II. Case 2- Large lateral defect

Extensive and asymmetrical defects can be reconstructed using both interpolation and mirroring techniques as shown in Figure 7. These methods leverage adjacent and symmetrical bone structures to estimate and reconstruct the missing regions effectively.

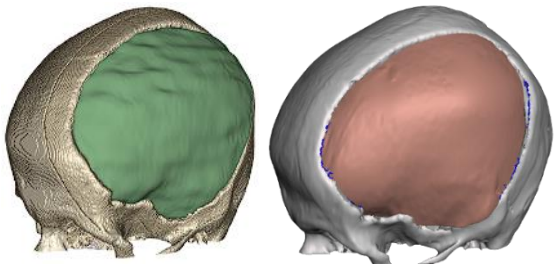

Figure 7: Implant for large lateral defects using top) mirroring and bottom) interpolation.

III.III. Case 3- Large bilateral defect

When the lesion crosses the skull's symmetry line, mirroring cannot be used to create the implant. When there is damage to the sagittal plane of the skull, Boolean subtraction cannot be done on a healthy site of the skull that is produced via mirroring, hence interpolation is performed as shown in Figure 8.

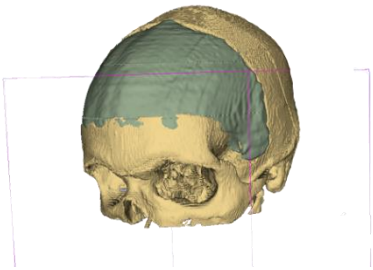

Figure 8: Implant for large bilateral defect using interpolation.

III.VI. Case 3- Large bilateral defect

When the contour of the cavity is unknown on DICOM images, interpolation is not feasible, so mirroring is performed instead, as shown in Figure 9.

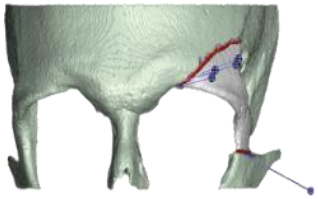

Figure 9: Implant for zygomatic bone defect using Mirroring.

III.V. Quantitative analysais

CloudCompare (version 2.10.1; GPL license), an open-source program was used to compare the two techniques quantitatively [31]. Therefore, the implant was positioned over the defect. This alignment was done manually at first, and then fine-tuned using CloudCompare's Iterative Closest Point (ICP) approach. To determine the implant fit, the distance between the implant and the defect was calculated. First, the distance from the implant was calculated using the deformed skull as a reference. After computation, the signed distance is returned. To compare the two approaches (mirroring and interpolation), the Edge Gradient Factor (EGF) is calculated. This factor is the ratio of the interpolated implant's mode edge deviation to the mirrored implant's mode edge deviation, as given in Equation 1.

Figures 10, 11, 12, and 13 show the EGF for all four cases where the defect is regenerated using both techniques (Figures 6-9), discussed in the previous sections. It is assumed that Mode edge deviation for interpolated implant be *I* and Mode edge deviation for mirrored implant be *M*, then (1) shows the formulae for Edge Gap Factor (EGF).

$$EGF = I / M \quad \text{.....(1)}$$

When the EGF is higher than 1, mirroring performs better than interpolation; when the EGF is lower than 1, interpolation performs better than mirroring; and when the EGF is equal to 1, both methods perform equally and may be used interchangeably to get the desired outcome [24].

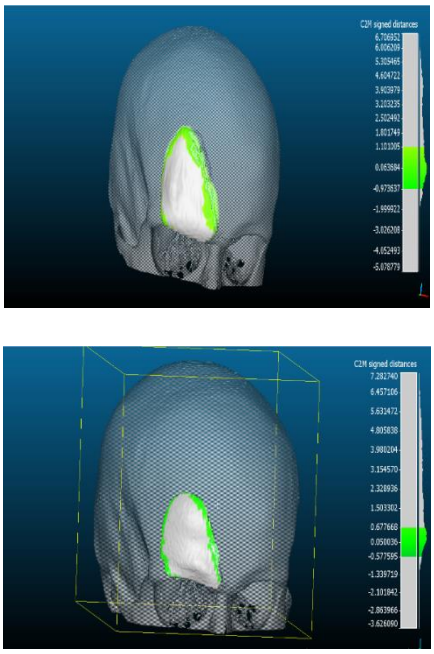

Figure 10: Distance measured between the edges of a small frontal defect and the implant created through top) Interpolation bottom) Mirroring for fitting.

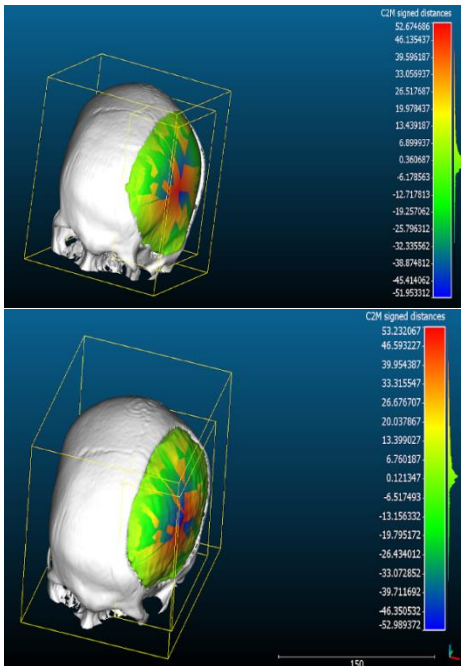

Figure 11: Distance measured between the edges of a large lateral defect and the implant created through top) Mirroring bottom) interpolation for fitting.

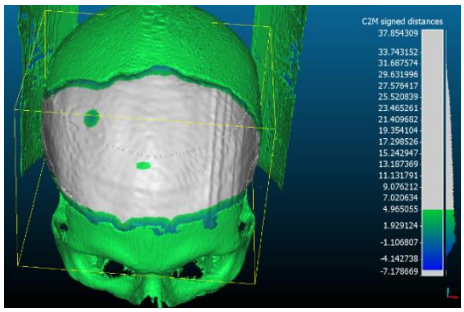

Figure 12: Distance measured between the edges of the defect and implant for large bilateral defect.

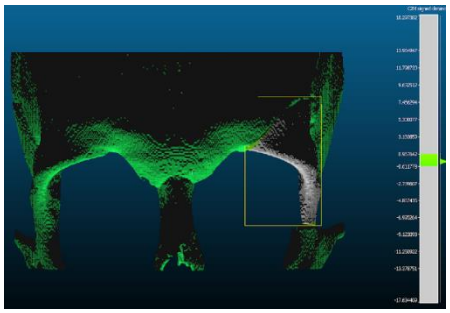

Figure 13: Distance measured between the edges of the defect and implant for Zygomatic bone defect.

IV. Discussion

The mirroring technique duplicates the corresponding healthy section from the opposite side of the skull, as a model for the mold. However, much of this assumes that the skull has ideal bilateral symmetry. Hence in case of a defect that crosses the sagittal plane, it is not possible to create and implant through mirroring alone. The other critique of this method is that most human skulls do not have ideal bilateral symmetry.

Therefore, mirrored implants may not have the same curvature as the original skull at the site of the defect. For this, manual adjustment is required post mirroring which makes this process heavily user-dependent, thus reducing the reproducibility of the process.

The interpolation technique originates the near-original geometry of the defected skull using the morphological contour interpolation method. Interpolation is done by first determining correspondence between shapes on adjacent segmented slices by detecting overlaps, then aligning the corresponding shapes, generating a transition sequence of one-pixel dilations, and taking the median as a result. Recursion is employed if the original segmented slices are separated by more than one empty slice. This class is n-dimensional and supports inputs of 3 or more dimensions. `Slices' are n-1-dimensional, and can be both automatically detected and manually set [12]. This method provides better reproducibility. In this paper, we present interpolation for every 5th slice as it provides a well-fitted implant without being computationally intensive.

Table 1: EGF for all 4 types of defects, regenerated using both mirroring and interpolation.

S. no.	Case	Type of defect	Mode edge distance for interpolated implant (I)	Mode edge distance for mirrored implant (M)	EGF (I/M)
1	Small frontal defect	Unilateral, small	0.063	0.050	1.260
2	Large lateral defect	Unilateral, large	0.121	0.360	0.336
3	Large bilateral defect	Bilateral, large	-1.106	NA	NA
4	Zygomatic bone defect	Unilateral, small	NA	-0.014	NA

Therefore, based on Table 1, in case - 1 (small frontal defect) we observed that mirroring has a higher performance as the EGF is greater than 1. For case 2 (large lateral defect) observed that interpolation had a higher performance as the EGF is less than 1. For case 3 (large bilateral defect) mirroring could not be used to produce an implant as the defect crossed the sagittal plane. Here only interpolation could be used, and the implant produced fits the defect to a satisfactory degree.

Since the zygomatic bone defect is located in a place where the CT scan cannot be utilized to identify the original skull's shape, interpolation cannot be used to manufacture an implant in case 4. All that could be done was mirroring, and the implant that was created sufficiently suits the deformity.

V. Protocol for cranial defect assessment and reconstruction technique selection

V.I Identification of cranial defect

The first step in cranial defect assessment involves categorizing the defect type:

a) Large Defects: Lateral Defect (case 2), Bilateral Defect (case 3)

i) Lateral Defect: Extensive and asymmetrical.

ii) Bilateral Defect: Spans both sides of the skull and crosses the sagittal plane.

b) Small Defects: Frontal Defect (case 1), Zygomatic Bone Defect (case 4)

i) Frontal Defect: Localized and non-sagittal.

ii) Zygomatic Bone Defect: Involves the zygomatic bone and is constrained by CT imaging limitations.

V.II Recommendation techniques based on EGF

Based on the calculated EGF values for all the defects as given in section 4, the following technique recommendations are made:

Large Defects: Use EGF to determine the best possible technique for defect regeneration, considering the symmetry of the defect with the intact portion of the skull.

i) Large Lateral Defects: Prefer interpolation if EGF < 1.

ii) Large Bilateral Defects: Use interpolation directly due to the sagittal plane crossing, as EGF is not available.

Small Defects: The optimal method for defect regeneration should be determined using EGF, considering the defect's size, symmetry with the healthy area of the skull, and computational constraints.

i) Small Frontal Defects: Use mirroring if EGF > 1.

ii) Zygomatic Bone Defects: Use mirroring directly due to CT imaging constraints, as EGF is not available.

This protocol offers a systematic approach to enhance cranial defect assessment and reconstruction technique selection, optimizing patient outcomes through precise implant fitting and effectiveness, as shown in Figure 14.

Therefore, based on the Table 1 presented above, in case - 1 (Small frontal defect) we observed that mirroring has a higher performance as the EGF is greater than 1.

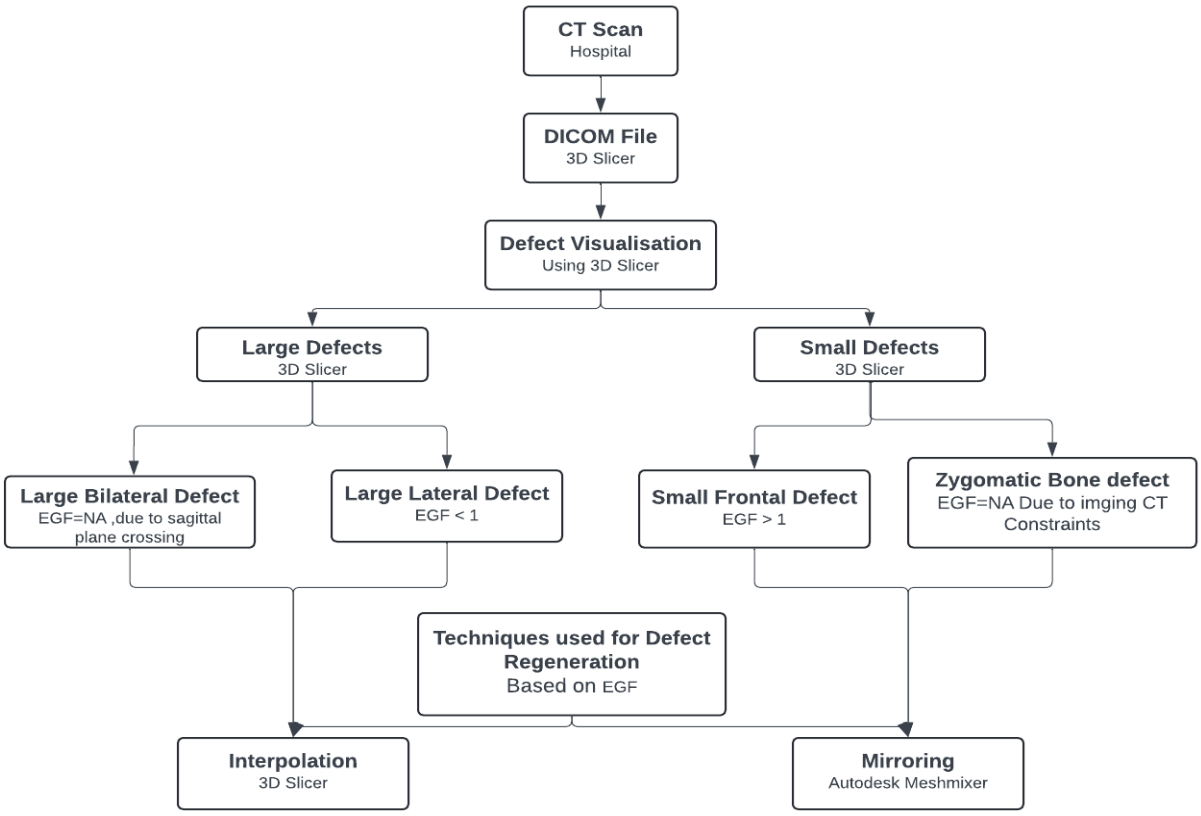

Figure 14: Methodical strategy to improve repair technique selection and cranial defect evaluation.

For case 2 (Large lateral defect) observed that interpolation had a higher performance as the EGF is less than 1.

For case 3 (Large bilateral defect) mirroring could not be used to produce an implant as the defect crossed the sagittal plane. Here only interpolation could be used, and the implant produced fits the defect to a satisfactory degree.

Since the zygomatic bone defect is located in a place where the CT scan cannot be utilized to identify the original skull's shape, interpolation cannot be used to manufacture an implant in case 4. All that could be done was mirroring, and the implant that was created sufficiently suits the deformity.

VI. Conclusion

A patient's quality of life following surgery is frequently determined by cranial reconstruction, making it a crucial moment in their care. Ensuring the physical integrity of the reconstructed skull is essential, but providing a strong basis for patients to return to their regular lives without undue anxiety is equally important. The mirrored approach replicates the matching healthy part from the opposing side of the skull, but this method assumes perfect bilateral symmetry, which is rarely the case. Interpolation techniques are crucial for accurate skull surface creation when the lesion crosses the sagittal plane or when bilateral symmetry is not perfect. However, interpolation requires significant computational resources and time. This study represents a noteworthy progression in cranial reconstruction, offering concrete advantages for patients, physicians, and the medical community. Using EGF, we can determine the best technique for precise defect regeneration for various defect types, thereby shortening the method selection process and improving the implant's resemblance to the real bone shape. Mirroring performed better for small frontal abnormalities when the EGF was greater than 1. Interpolation worked better for big lateral flaws when EGF was less than one. In the instance of major bilateral deficiencies that crossed the sagittal plane, only interpolation could be employed, and the implant created was excellent. Mirroring was the only viable alternative for zygomatic bone deformities, when CT scans could not determine the original skull shape, and the implant developed was suitable for the abnormality. As a result, this study offers a strategy for defect regeneration based on the kind of defect that a surgeon might use to achieve precise implant production with better fit.

Acknowledgements

The authors are grateful to Nottingham Trent University International Partnership Fund (IPF) scheme for funding this research. Ministry of Education (MoE), Government of India, Grant number: (17-11/2015-PN-1) for funding this project under Design Innovation Centre (DIC) subtheme Medical Devices & Restorative Technologies.

Author's Statement

The authors confirm that there are no known conflicts of interest associated with this publication and there has been no financial support for this work that could have influenced its outcome. Informed consent: Informed consent has been obtained from all individuals included in this

study. Ethical approval: The research related to human use complies with all the relevant national regulations, institutional policies and was performed in accordance with the tenets of the Helsinki Declaration and has been approved by the authors' institutional review board or equivalent committee.

REFERENCES

[1] S. Andrabi, A. Sarmast, A. Kirmani, and A. Bhat, "Cranioplasty: Indications, procedures, and outcome - An institutional experience," Surg Neurol Int, vol. 8, no. 1, 2017, doi: 10.4103/sni.sni_45_17.

[2] World Health Organization Injuries and Violence. [(accessed on 16 February 2023)]. Available online: https://www.who.int/news-room/fact-sheets/detail/injuries-and-violence

[3] de Vries LS, Gunardi H, Barth PG, Bok LA, Verboon-Maciolek MA, Groenendaal F. The spectrum of cranial ultrasound and magnetic resonance imaging abnormalities in congenital cytomegalovirus infection. Neuropediatrics. 2004 Apr;35(2):113-9. doi: 10.1055/s-2004-815833. PMID: 15127310

[4] Osenbach, R. K. "Central Nervous System İnfections in: Grossman RG and Loftus CM (Eds) Principles of Neurosurgery." (1999): 246.

[5] Mayfield Brain & Spine, Brain Tumors: An introduction. [(accessed on 18 February 2023)]. Available online: https://mayfieldclinic.com/pe-braintumor.htm

[6] Ridgway EB, Weiner HL. Skull deformities. Pediatr Clin North Am. 2004 Apr;51(2):359-87. doi: 10.1016/j.pcl.2003.12.001. PMID: 15062675.

[7] Gerstl JVE, Rendon LF, Burke SM, Doucette J, Mekary RA, Smith TR. Complications and cosmetic outcomes of materials used in cranioplasty following decompressive craniectomy-a systematic review, pairwise meta-analysis, and network meta-analysis. Acta Neurochir (Wien). 2022 Dec;164(12):3075-3090. doi: 10.1007/s00701-022-05251-5. Epub 2022 May 20. PMID: 35593924.

[8] Thimukonda Jegadeesan J, Baldia M, Basu B. Next-generation personalized cranioplasty treatment. Acta Biomater. 2022 Dec;154:63-82. doi: 10.1016/j.actbio.2022.10.030. Epub 2022 Oct 19. PMID: 36272686.

[9] Ulmeanu ME, Mateș IM, Doicin CV, Mitrică M, Chirteș VA, Ciobotaru G, Semenescu A. Bespoke Implants for Cranial Reconstructions: Preoperative to Postoperative Surgery Management System. Bioengineering (Basel). 2023 Apr 29;10(5):544. doi: 10.3390/bioengineering10050544. PMID: 37237614; PMCID: PMC10215819.

[10] Niinomi M, Liu Yi, Nakai M, Liu H, Li H (2016) Biomedical Titanium alloys with Young's moduli close to that of cortical bone. Regenerative Biomaterials 3(3):173–185. https://doi.org/10.1093/rb/rbw016

[11] Mian, Syed Hammad & Moiduddin, Khaja & Abdo, Basem & Sayeed, Abdul & Alkhalefah, Hisham. (2022). Modeling and evaluation of meshed implants for cranial reconstruction. The International Journal of Advanced Manufacturing Technology. 118. 10.1007/s00170-021-08161-5.

[12] Galarraga H, Lados D, Dehof R, KirkaNandwana MP (2016) Effects of the microstructure and porosity on properties of Ti-6Al-4V ELI alloy fabricated by electron beam melting (EBM). Addit Manuf 10(February):57. H

[13] Bidaux, Jacques-Eric, J. García-Gómez, H. Hamdan, D. Zuferey, Mikel Rodríguez-Arbaizar, Hervé Girard, and Efrain CarrenoMorelli. 2011. "Tape casting of porous titanium thin sheets from titanium hydride." In Proceedings of the Euro International Powder Metallurgy Congress and Exhibition, Euro PM 2011. Vol. 2. Barcelona, Spain: Euro PM2011 – Cellular Materials.

[14] Reig L, Tojal C, Busquets D, Amigó V (2013) Microstructure and mechanical behavior of porous Ti–6Al–4V processed by spherical powder sintering. Materials 6(10):4868–4878

[15] Xu X, Nash P, Mangabhai D (2017) Characterization and sintering of armstrong process titanium powder. JOM 69(4):770–775.

[16] Vividha V, Krishnan M, Kumar M P S, Murugan P S, Rajamanickam P. Multidisciplinary Approach to Patient-Specific Implants (PSIs): A Case Report and Review of Literature. Cureus. 2023 June 30;15(6):e41238. doi: 10.7759/cureus.41238. PMID: 37529522; PMCID: PMC10387731.

[17] Mishra A, Khatri M, Bansal M, Mohd. Rehhan, Gaind S, Khan S. Changing trends in implant designs: A review. IP Int J Periodontol Implantol 2023;8(3):117-123.

[18] Bogu, V. Phanindra, Y. Ravi Kumar, and Asit Kumar Khanara. "Modeling and structural analysis of skull/cranial implant: beyond midline deformities." Acta of Bioengineering and Biomechanics 19.1 (2017): 125-131.

[19] Gall, M., Li, X., Chen, X., Schmalstieg, D. and Egger, J., 2016, August. Computer-aided planning and reconstruction of cranial 3D implants. In 2016 38th Annual International Conference of the IEEE Engineering in Medicine and Biology Society (EMBC) (pp. 1179-1183). IEEE.

[20] Scolozzi, P., 2012. Maxillofacial reconstruction using polyetheretherketone patient-specific implants by "mirroring" computational planning. Aesthetic plastic surgery, 36(3), pp.660-665.

[21] Singare, S., Lian, Q., Wang, W.P., Wang, J., Liu, Y., Li, D. and Lu, B., 2009. Rapid prototyping assisted surgery planning and custom implant design. Rapid Prototyping Journal.

[22] Abdullah, J.Y., Abdullah, A.M., Hueh, L.P., Husein, A., Hadi, H. and Rajion, Z.A., 2021. Cranial Implant Design Applying Shape-Based Interpolation Method via Open-Source Software. Applied Sciences, 11(16), p.7604.

[23] Filipe M. M. Marreiros, Yann Heuzé, Michael Verius, Claudia Unterhofer, Wolfgang Freysinger, et al.. Custom implant design for large cranial defects. International Journal of Computer Assisted Radiology and Surgery, Springer Verlag, 2016, pp.14. ff10.1007/s11548-016-1454-8ff. Ffhal-01842538f

[24] Jindal, P., Bhattacharya, A., Singh, M., Pareek, D., Watson, J., O'Connor, R., Breedon, P., Reinwald, Y. and Juneja, M., 2022. Unilateral cranial defect bone reconstruction utilizing 3D design and manufacturing. Transactions on Additive Manufacturing Meets Medicine, 4 (1): 655. ISSN 2749-3229

[25] Jindal P, Bharadwaja SSS, Rattra S, et al. Designing cranial fixture shapes and topologies for optimizing PEEK implant thickness in cranioplasty. Proceedings of the Institution of Mechanical Engineers, Part L: Journal of Materials: Design and Applications. 2023;237(8):1752-1770. doi:10.1177/14644207231155761

[26] Juneja M, Chawla J, Dhingra G, et al. Analysis of additive manufacturing techniques used for maxillofacial corrective surgeries. Proceedings of the Institution of Mechanical Engineers, Part C: Journal of Mechanical Engineering Science. 2022;236(14):7864-7875. doi:10.1177/09544062221081992

[27] Kamalian, S., Lev, M.H. and Gupta, R., 2016. Computed tomography imaging and angiography–principles. Handbook of clinical neurology, 135, pp.3-20.

[28] Szilvśi-Nagy, M. and Matyasi, G.Y., 2003. Analysis of STL files. Mathematical and computer modeling, 38(7-9), pp.945-960.

[29] Jindal, Prashant & Bharadwaja, Shreerama & Rattra, Shubham & Pareek, Deval & Gupta, Vipin & Breedon, Philip & Reinwald, Yvonne & Juneja, Mamta. (2022). Optimizing cranial implant and fixture design using different materials in cranioplasty. Proceedings of the Institution of Mechanical Engineers, Part L: Journal of Materials: Design and Applications. 237. 146442072211048. 10.1177/14644207221104875

[30] Gill, Deepkamal & Walia, Kartikeya & Rawat, Aditi & Bajaj, Divya & Gupta, Vipin & Gupta, Anand & Juneja, Mamta & Tuli, Rakesh & Jindal, Prashant. (2018). 3D modeling and printing of craniofacial implant template. Rapid Prototyping Journal. 25. 10.1108/RPJ-12-2017-0257.

[31] CloudCompare. (version 2.10.1) [GPL Software]. Available online: https://www.danielgm.net/cc/